

Synthesis, characterization and catalytic activity in the carbonylation of ethene of  $cis$ -[Pd(H<sub>2</sub>O)<sub>2</sub>(PPh<sub>3</sub>)<sub>2</sub>]X<sub>2</sub> · nH<sub>2</sub>O (X = *p*-CH<sub>3</sub>C<sub>6</sub>H<sub>4</sub>SO<sub>3</sub>, n = 2; X = CH<sub>3</sub>SO<sub>3</sub>, n = 0). X-ray structure of  $cis$ -[Pd(H<sub>2</sub>O)<sub>2</sub>(PPh<sub>3</sub>)<sub>2</sub>](*p*-CH<sub>3</sub>C<sub>6</sub>H<sub>4</sub>SO<sub>3</sub>)<sub>2</sub> · 2H<sub>2</sub>O and of  $cis$ -[Pd(H<sub>2</sub>O)<sub>2</sub>(PPh<sub>3</sub>)<sub>2</sub>](CH<sub>3</sub>SO<sub>3</sub>)<sub>2</sub> · 2CH<sub>2</sub>Cl<sub>2</sub>

Gianni Cavinato <sup>a</sup>, Andrea Vavasori <sup>b</sup>, Luigi Toniolo <sup>b,\*</sup>, Alessandro Dolmella <sup>c</sup>

<sup>a</sup> Department of Chemistry Science, University of Padua, via Marzolo 1, 35100 Padua, Italy

<sup>b</sup> Department of Chemistry, University of Venice, Dorsoduro 2137, 30123 Venice, Italy

<sup>c</sup> Department of Pharmaceutical Science, University of Padua, via Marzolo 5, 35131 Padua, Italy

Received 28 February 2004; accepted 23 April 2004

Available online 15 June 2004

## Abstract

The complexes  $cis$ -[Pd(H<sub>2</sub>O)<sub>2</sub>(PPh<sub>3</sub>)<sub>2</sub>]X<sub>2</sub> · nH<sub>2</sub>O (**Ia**: X = *p*-CH<sub>3</sub>C<sub>6</sub>H<sub>4</sub>SO<sub>3</sub>, n = 2; **Ia**: X = CH<sub>3</sub>SO<sub>3</sub>, n = 0) have been synthesized by reacting Pd(OAc)<sub>2</sub>, PPh<sub>3</sub> and HX in acetone in the presence of H<sub>2</sub>O. They have been characterized by IR, <sup>1</sup>H and <sup>31</sup>P NMR spectroscopy and TA analysis. By re-crystallization of these complexes, crystals of **Ia** and **Ia** · 2CH<sub>2</sub>Cl<sub>2</sub> suitable for the X-ray analysis have been obtained. The solid-state investigation of **Ia** reveals that the two *p*-toluenesulfonato units act as counter anions of a dicationic complex, in which the metal atom is surrounded in a square planar environment realized by two water molecules and two PPh<sub>3</sub> moieties that are *cis* to each other. The X-ray investigation of **Ia** · 2CH<sub>2</sub>Cl<sub>2</sub> shows that also in this case the two PPh<sub>3</sub> are *cis* to each other and that in the acentric triclinic cell there are two independent [Pd(H<sub>2</sub>O)<sub>2</sub>(PPh<sub>3</sub>)<sub>2</sub>]<sup>2+</sup> units, together with two methanesulfonato counter anions and two crystallization molecules of CH<sub>2</sub>Cl<sub>2</sub>. The cationic complexes **Ia** and **Ia** are easily *inter*-converted with the neutral species *trans*-[Pd(*p*-CH<sub>3</sub>C<sub>6</sub>H<sub>4</sub>SO<sub>3</sub>)<sub>2</sub>(PPh<sub>3</sub>)<sub>2</sub>] (**Ib**) and *trans*-[Pd(CH<sub>3</sub>SO<sub>3</sub>)<sub>2</sub>(PPh<sub>3</sub>)<sub>2</sub>] (**Ib**), respectively, depending on temperature and solvent. In chloroform at r.t., complex **Ia** catalyzes the carbonylation of ethene to a polyketone; at higher temperature in methanol it catalyzes the hydroesterification of ethene. In both cases catalysis is accompanied by CO<sub>2</sub> evolution. These results suggest that catalysis occurs via initial formation of a Pd(II)–H species by interaction of H<sub>2</sub>O with CO on the metal center though a reaction closely related to that of the water gas-shift.

© 2004 Elsevier B.V. All rights reserved.

**Keywords:** Palladium; Phosphine; Aqua; Complexes; *Cis*-geometry; Catalyst; Carbonylation; Olefin; Polyketone; Ester

## 1. Introduction

Pd(II)–phosphine complexes in which the cationic charge is balanced by weakly coordinating anions readily displaceable by the reagents are efficient cata-

lysts for the carbonylation of olefins [1,2]. A wide spectrum of products can be obtained. For example, when ethene is carbonylated in MeOH, the products range from methyl propanoate to oligomeric or high molecular weight perfectly alternated polyketones [3]. The first highly efficient catalyst system that produced a polyketone was prepared by Drent et al. [4,5], of Shell Co., from equimolar amount of [Pd(AcO)<sub>2</sub>] and 1,3-bis(diphenylphosphine)propane together with two equivalents of a Bronsted acid, such as *p*-CH<sub>3</sub>C<sub>6</sub>H<sub>4</sub>SO<sub>3</sub>H or HBF<sub>4</sub>, which displaces the acetate anion

\* Corresponding author. Tel.: +390-41-2348553; fax: +390-41-2348517.

E-mail address: [toniolo@unive.it](mailto:toniolo@unive.it) (L. Toniolo).

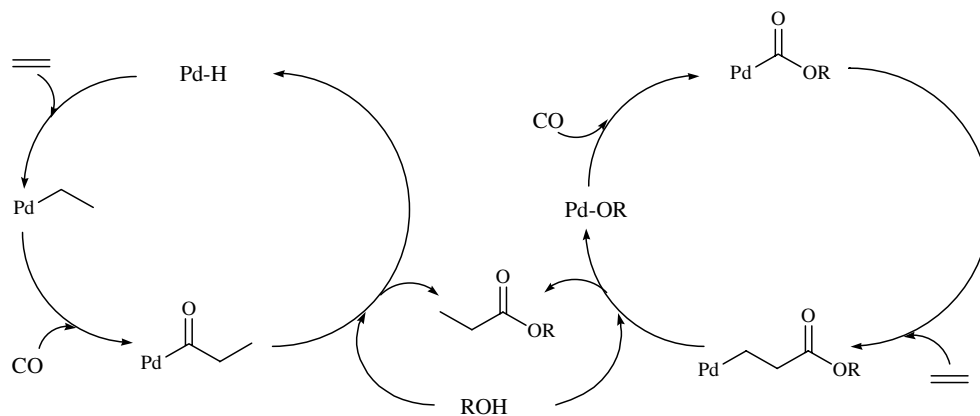
with formation of a cationic complex having coordination sites readily available to the monomers. In contrast, the catalyst prepared from  $[\text{Pd}(\text{AcO})_2]$ , an excess of  $\text{PPh}_3$  and of a Bronsted acid, produced selectively propanoate [5]. It was proposed that the striking difference in selectivity is related to the coordination geometry of the ligands. The chelating diphosphine ligand imposes a *cis* geometry also for the growing polymeric chain and the site that coordinates the monomer, thus favoring the multiple insertion steps that bring to the polyketone [1]. In the other case, the insertion of the monomer is also favored when the two phosphine ligands are in *cis* position, however, once an alkyl or acyl palladium intermediate forms, the preferred geometry is that with the two phosphine ligands in *trans* position in order to avoid the unfavorable occurrence of a Pd–P bond *trans* a Pd–C bond. Hence, chain growth becomes unfavorable and termination occurs just after only one molecule of each monomer inserts, thus resulting in the production of propanoate [1]. However, at low temperature the *cis*–*trans* isomerization is slow, or even suppressed, and polymerization can occur also with Pd– $\text{PPh}_3$  based catalysts, as found using the series of precursors  $[\text{Pd}(\text{PPh}_3)_n(\text{CH}_3\text{CN})_{4-n}](\text{BF}_4)$  ( $n = 1$ –3) at r.t., in aprotic solvents such as chloroform [6–8]. The active Pd–H species initiating the catalysis probably forms from the interaction of Pd(II) with protic impurities or is related to the observed catalytic dimerization of  $\text{C}_2\text{H}_4$  in the absence of CO [7]. It was proposed that internal coordination of Pd with a carbonyl oxygen of the growing chain maintains the *cis* geometry that favors the polymerization [1].

Recently, we extended the studies on the hydroesterification of olefins using the catalytic system based on  $\text{Pd}(\text{AcO})_2/p\text{-CH}_3\text{C}_6\text{H}_4\text{SO}_3\text{H}/\text{PPh}_3$  originally employed

by Drent [9–14]. Pd(II)–hydrido and -acyl species were detected by NMR spectroscopy [10]. Moreover, it has been found that the catalytic activity is significantly enhanced when catalysis is carried out in the presence of a hydride source, such as  $\text{H}_2\text{O}$ ,  $p\text{-CH}_3\text{C}_6\text{H}_4\text{SO}_3\text{H}$ ,  $\text{H}_2$ . It has been proposed that of the two widely accepted mechanisms (Scheme 1), one via initial formation of a Pd(II)–H species, followed by subsequential insertion of the olefin and of CO, with formation of a Pd(II)–acyl intermediate, which undergoes alkanol attack with production of the ester and regeneration of the Pd(II)–hydride [15,16], and the other one via initial formation of a Pd(II)–COOR species, followed by insertion of the olefin and by protonolysis of the resulting Pd(II)–alkyl intermediate [17–19], the first one plays a major role [9,11–13]. Further support to this suggestion came very recently from the catalytic activity of the acyl complex *trans*- $[\text{Pd}(\text{COEt})(p\text{-CH}_3\text{C}_6\text{H}_4\text{SO}_3)(\text{PPh}_3)_2]$ , isolated in the course of the methoxycarbonylation of ethene [14].

The precursor system was also investigated in solution. In polar solvents, like methanol, the in situ generated species from  $[\text{Pd}(\text{AcO})_2]/\text{PPh}_3/p\text{-CH}_3\text{C}_6\text{H}_4\text{SO}_3\text{H} = 1/4/10$ , as evidenced by  $^{31}\text{P}$  NMR analysis, are  $[\text{Pd}(p\text{-CH}_3\text{C}_6\text{H}_4\text{SO}_3)_2(\text{PPh}_3)_2]$ ,  $[\text{Pd}(\text{H}_2\text{O})_2(\text{PPh}_3)_2](p\text{-CH}_3\text{C}_6\text{H}_4\text{SO}_3)_2$ , and  $[\text{Pd}(\text{PPh}_3)_3](p\text{-CH}_3\text{C}_6\text{H}_4\text{SO}_3)_2$  [10]. Up to now scarce attention has been paid to the geometry of the species generated from the precursor, although it may be of paramount importance on influencing the catalytic activity and selectivity.

In this paper, we report the synthesis, characterization of the title complexes, the catalytic activity in the carbonylation of ethene of **Ia** and of **IIa** and the X-ray structures of *cis*- $[\text{Pd}(\text{H}_2\text{O})_2(\text{PPh}_3)_2](p\text{-CH}_3\text{C}_6\text{H}_4\text{SO}_3)_2 \cdot 2\text{H}_2\text{O}$  and of *cis*- $[\text{Pd}(\text{H}_2\text{O})_2(\text{PPh}_3)_2](\text{CH}_3\text{SO}_3)_2 \cdot 2\text{CH}_2\text{Cl}_2$  (**IIa** $2\text{CH}_2\text{Cl}_2$ ).



Scheme 1. Pd(II)–hydride and Pd(II)–carbomethoxy catalytic cycles.

## 2. Experimental

### 2.1. Materials

Methanol (purity >99.5%, 0.01% of water), *n*-hexane, *n*-pentane, CH<sub>2</sub>Cl<sub>2</sub>, diethyl ether, toluene, acetone (H<sub>2</sub>O = 0.5%) and deuterated solvents CD<sub>3</sub>COCD<sub>3</sub>, C<sub>6</sub>D<sub>6</sub>, and CDCl<sub>3</sub> were purchased from Aldrich; Pd(OAc)<sub>2</sub>, *p*-CH<sub>3</sub>C<sub>6</sub>H<sub>4</sub>SO<sub>3</sub>H · H<sub>2</sub>O, CH<sub>3</sub>SO<sub>3</sub>H and PPh<sub>3</sub> were Fluka products. Carbon monoxide and ethene were supplied by SIAD Company ('research grade', purity >99.9%). The complexes [Pd(*p*-CH<sub>3</sub>C<sub>6</sub>H<sub>4</sub>SO<sub>3</sub>)<sub>2</sub>(PPh<sub>3</sub>)<sub>2</sub>], *trans*-[Pd(COCH<sub>2</sub>CH<sub>3</sub>)(*p*-CH<sub>3</sub>C<sub>6</sub>H<sub>4</sub>SO<sub>3</sub>)(PPh<sub>3</sub>)<sub>2</sub>] and *trans*-[Pd(COCH<sub>2</sub>CH<sub>3</sub>)Cl(PPh<sub>3</sub>)<sub>2</sub>] were prepared according to the methods reported in the literature [10,14,16].

### 2.2. General procedure

The IR spectra were recorded in nujol mull on a Nicolet FT-IR instruments mod Nexus. <sup>1</sup>H and <sup>31</sup>P NMR spectra of complexes were recorded on a Bruker AMX 300 spectrometer equipped with a BB multinuclear probe operating in the FT mode at 300 and 121.442 MHz for <sup>1</sup>H and <sup>31</sup>P, respectively; samples examined were dissolved in CD<sub>3</sub>COCD<sub>3</sub>, C<sub>6</sub>D<sub>6</sub> or CDCl<sub>3</sub>. The <sup>1</sup>H and <sup>13</sup>C NMR spectra of the polyketone were recorded on a Bruker Avance 300 spectrometer in 1,1,1,3,3,3-hexafluoroisopropanol/CDCl<sub>3</sub> (10/1) using the Inverse <sup>1</sup>H-gated decoupling technique.

Products of the hydroesterification reaction were analyzed by GC on a HP 5890 series II instrument equipped with a 30 m × 0.53 mm × 0.1 μm HP 5 column. The gas-phase analysis for CO<sub>2</sub> was performed using a 5.5 m × 3.8 mm SS Silica Gel, 60/80 packed column (detector: TCD; carrier gas: helium, 30 ml/min; oven: 40 °C (2 min) to 100 °C at 15 °C/min).

Thermogravimetric analysis was performed using a TA instrument model SDT 2960 simultaneous DSC-TGA. The sample, **Ia** or **IIa** (5 mg), was placed on the dish and heated from 25 to 130 °C at 7 °C/min with a nitrogen flow of 30 ml/min.

The catalytic carbonylation of ethene to polyketone was carried out using a magnetically stirred autoclave of ca. 50 ml capacity. The catalytic methoxycarbonylation of ethene was carried out in a stainless steel autoclave of ca. 250 ml of capacity, provided with a self-aspirating turbine. In both cases, in order to prevent contamination by metallic species, due to corrosion of the internal surface of the autoclave, the catalyst was added to the solvent in a glass bottle or a teflon-beaker placed into the autoclave. The solvent was degassed at r.t. with a mixture of CO/C<sub>2</sub>H<sub>4</sub> before adding the catalytic precursor. The autoclave was washed by pressurizing with a 1/1 mixture of CO/C<sub>2</sub>H<sub>4</sub> (ca. 0.5 MPa) and then depressurizing to atmospheric pressure (this cycle was repeated 5 times, at

room temperature with stirring). After washing, a gas sample was analyzed by GC: no CO<sub>2</sub> was detected. During the reaction CO–ethene mixture (1/1) was supplied from a gas reservoir connected to the autoclave through a constant pressure regulator. The autoclave was provided with a temperature control (±0.5 K).

### 2.3. Synthesis of *cis*-[Pd(H<sub>2</sub>O)<sub>2</sub>(PPh<sub>3</sub>)<sub>2</sub>](*p*-CH<sub>3</sub>C<sub>6</sub>H<sub>4</sub>SO<sub>3</sub>)<sub>2</sub> · 2H<sub>2</sub>O (**Ia**) and of *cis*-[Pd(H<sub>2</sub>O)<sub>2</sub>(PPh<sub>3</sub>)<sub>2</sub>](CH<sub>3</sub>SO<sub>3</sub>)<sub>2</sub> (**IIa**) complexes

Upon addition, dropwise and under vigorous stirring, of a PPh<sub>3</sub> acetone solution (2.1 mmol in 3 ml) to a Pd(OAc)<sub>2</sub> acetone solution (1 mmol in 10 ml), a pale yellow solid precipitated, which dissolved by dropping an acetone solution of *p*-CH<sub>3</sub>C<sub>6</sub>H<sub>4</sub>SO<sub>3</sub>H · H<sub>2</sub>O (2.1 mmol, 2 ml). Addition of *n*-hexane (20 ml) caused precipitation of a pale yellow solid. After filtration the solid was washed with *n*-hexane and diethyl ether and dried under vacuum. Yield 90% of **Ia**.

Yellow-orange crystals of **Ia**, suitable for X-ray diffraction studies, have been obtained by recrystallization from *n*-hexane–CH<sub>2</sub>Cl<sub>2</sub> at –10 °C.

Following the same procedure just reported, but adding the acid CH<sub>3</sub>SO<sub>3</sub>H (2.1 mmol in 3 ml of acetone) in place of *p*-CH<sub>3</sub>C<sub>6</sub>H<sub>4</sub>SO<sub>3</sub>H, complex **IIa** was obtained in 90% yield.

Recrystallization of **IIa** from *n*-pentane–CH<sub>2</sub>Cl<sub>2</sub> at –10 °C gave yellow-orange crystals of **IIa** · 2CH<sub>2</sub>Cl<sub>2</sub> suitable for X-ray diffraction studies.

Complexes **Ia** and **IIa** have been obtained in high yield (90%) also from preformed [Pd(OAc)<sub>2</sub>(PPh<sub>3</sub>)<sub>2</sub>] following the procedure just described.

### 2.4. Interconversion of **Ia** and **IIa** to [Pd(*p*-CH<sub>3</sub>C<sub>6</sub>H<sub>4</sub>SO<sub>3</sub>)<sub>2</sub>(PPh<sub>3</sub>)<sub>2</sub>] (**Ib**) and to [Pd(CH<sub>3</sub>SO<sub>3</sub>)<sub>2</sub>(PPh<sub>3</sub>)<sub>2</sub>] (**IIb**)

By adding *n*-hexane to a toluene solution of **Ia** or **IIa** warmed at 60 °C, complexes **Ib** and **IIb** have been obtained as pale yellow solids (yield 85%). **Ia** and **IIa** are reobtained by adding *n*-hexane to an acetone solution of **Ib** or **IIb** at r.t.

### 2.5. Carbonylation of ethene to polyketone

The carbonylation was carried out at r.t. In a typical experiment, complex **Ia** (0.1 mmol) was dissolved in 10 ml of CHCl<sub>3</sub> containing four equivalents of CH<sub>3</sub>CN. After purging the autoclave to eliminate traces of air and of CO<sub>2</sub>, it was charged with 4.5 MPa of CO/ethene 1/1. After 20 h, reaction the gas phase was analyzed. CO<sub>2</sub> was unambiguously detected by GC. The autoclave was then depressurized and opened. The white solid polyketone was filtered, washed with CHCl<sub>3</sub> and diethylether and dried under vacuum at 60 °C.

## 2.6. Methoxycarbonylation of ethene

In a typical experiment, 1 mmol of **Ia** together with PPh<sub>3</sub> and *p*-CH<sub>3</sub>C<sub>6</sub>H<sub>4</sub>SO<sub>3</sub>H (1/6/8) was dissolved in 50 ml of CH<sub>3</sub>OH in a teflon beaker. After purging the autoclave, it followed the procedure already described in the literature [11]. After 2 h, reaction at 80 °C under 4.5 MPa (CO/ethene = 1/1), the gas phase was analyzed by GC: CO<sub>2</sub> was present. The autoclave was then cooled and depressurized. The content of the beaker was analyzed by GC (TOF = 420 mol of methyl propanoate/per mol of **Ia/h**).

## 2.7. X-ray data collection, structure solution and refinement

The X-ray crystal structure determinations of the complexes **Ia** and **IIa** · 2CH<sub>2</sub>Cl<sub>2</sub> were carried out at room temperature with a STADI 4 CCD STOE area detector diffractometer, using for both samples a single-crystal mounted in a thin-walled glass capillary with graphite-monochromated Mo K $\alpha$  radiation ( $\lambda = 0.71073$  Å). A summary of the crystal and refinement data is shown in Table 1.

The structure of both complexes was solved by the heavy-atom methods and the refinement procedure was

Table 1  
Crystal and refinement data for **Ia** and **IIa** · 2CH<sub>2</sub>Cl<sub>2</sub>

Complex	<b>Ia</b>	<b>IIa</b> · 2CH <sub>2</sub> Cl <sub>2</sub>
Formula	C <sub>50</sub> H <sub>52</sub> O <sub>10</sub> P <sub>2</sub> S <sub>2</sub> Pd	C <sub>40</sub> H <sub>44</sub> Cl <sub>4</sub> O <sub>8</sub> P <sub>2</sub> S <sub>2</sub> Pd
Molecular weight	1045.4	1027.01
Color	colorless	yellow
Crystal system	triclinic	triclinic
Space group	<i>P</i> $\bar{1}$ (No. 2)	<i>P</i> 1 (No. 1)
<i>a</i> (Å)	12.432(3)	12.099(2)
<i>b</i> (Å)	12.740(3)	12.622(3)
<i>c</i> (Å)	15.966(3)	18.461(4)
$\alpha$ (°)	79.66(3)	93.45(3)
$\beta$ (°)	89.69(3)	103.04(3)
$\gamma$ (°)	78.63(3)	99.77(3)
<i>V</i> (Å <sup>3</sup> )	2437(1)	2247.4(8)
<i>Z</i>	2	2
<i>D</i> <sub>calc</sub> (g cm <sup>-3</sup> )	1.424	1.518
<i>F</i> (000)	1080	1048
Crystal dimensions (mm)	0.25 × 0.25 × 0.25	0.20 × 0.10 × 0.10
$\theta$ limits (°)	3.5/29.6	3.6/26.1
Number of independent data	9270	7860
Number of data with <i>I</i> > 2 $\sigma$ ( <i>I</i> )	4275	3229
Number of variables	586	547
<i>R</i> ( <i>F</i> ) <sup>a</sup>	0.044	0.0897
<i>wR</i> ( <i>F</i> <sup>2</sup> ) <sup>b</sup>	0.055	0.2030
Largest peak in $\Delta F$ (e Å <sup>-3</sup> )	0.355	1.081
Goodness-of-fit (GOF) <sup>c</sup>	0.747	0.838

$$^a R(F) = \sum ||F_o| - |F_c|| / \sum |F_o|$$

$$^b wR(F^2) = [\sum w(|F_o|^2 - |F_c|^2)^2 / \sum w(|F_o|^2)^2]^{1/2}$$

$$^c GOF = [\sum w(|F_o|^2 - |F_c|^2)^2 / (n - p)]^{1/2}$$

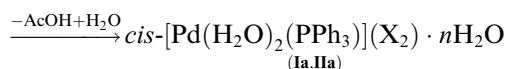
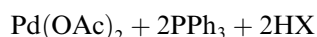
performed by full-matrix least-squares based on *F*<sup>2</sup>. In complex **Ia**, the non-hydrogen atoms were assigned anisotropic displacement parameters and the hydrogen atoms were treated by means of a riding model. The final Fourier difference maps did not show any feature; the largest maximum, less than half an electron, being close to O(1).

Unfortunately, the results obtained for complex **IIa** · 2CH<sub>2</sub>Cl<sub>2</sub> were far from optimal. The crystal proved very sensitive towards X-rays, degraded very rapidly and decomposed dramatically after only 4 h of irradiation. Accordingly, it was impossible to perform any absorption correction and, worst of all, it was also impossible to utilize diffraction data of high quality for the refinement procedure and only Pd, Cl, S and P atoms were assigned anisotropic displacement parameters. The largest maxima of the final Fourier difference map, located close to Pd(1) and Pd(2), were just more than one electron. All calculations were made with the SHELXTL/PC [20] and SHELXL-93 [21] suite of programs.

## 3. Results and discussion

### 3.1. Characterization of **Ia**, **IIa**, **Ib** and **IIb**

Complexes **Ia** and **IIa** were synthesized by reacting Pd(OAc)<sub>2</sub>, PPh<sub>3</sub> and HX (X = *p*-CH<sub>3</sub>C<sub>6</sub>H<sub>4</sub>SO<sub>3</sub>, CH<sub>3</sub>SO<sub>3</sub>) in acetone



(**Ia**: X = *p*-CH<sub>3</sub>C<sub>6</sub>H<sub>4</sub>SO<sub>3</sub>, *n* = 2; **IIa**: X = CH<sub>3</sub>SO<sub>3</sub>, *n* = 0; **Ib**, X = *p*-CH<sub>3</sub>C<sub>6</sub>H<sub>4</sub>SO<sub>3</sub>; **IIb**, X = CH<sub>3</sub>SO<sub>3</sub>).

As reported in Section 2, the aqua complexes easily interconvert with the anhydrous ones depending on solvent and temperature.

Elemental analysis, IR and NMR data are reported in Table 2. The IR spectrum of both **Ia** and **IIa** shows two broad absorptions at 3508, 3445 cm<sup>-1</sup> and 3534, 3489 cm<sup>-1</sup>, respectively, assigned to  $\nu_{\text{as}}(\text{O-H})$  and  $\nu_{\text{s}}(\text{O-H})$  of the water molecules [13,22–25]. The absorptions at 1227, 1033, 1008 cm<sup>-1</sup> and at 1233, 1036, 1009 cm<sup>-1</sup> are characteristic of the -SO<sub>3</sub><sup>-</sup> group of the anions *p*-CH<sub>3</sub>-C<sub>6</sub>H<sub>4</sub>SO<sub>3</sub><sup>-</sup> and CH<sub>3</sub>SO<sub>3</sub><sup>-</sup> [13,26–28].

The <sup>31</sup>P NMR spectrum shows a singlet at ca. 34 ppm, close to 39.05 ppm for *cis*-[Pd(H<sub>2</sub>O)<sub>2</sub>(PPh<sub>3</sub>)<sub>2</sub>](CF<sub>3</sub>SO<sub>3</sub>)<sub>2</sub> in acetone [29]. The <sup>1</sup>H NMR spectrum of **Ia** shows singlets at 2.30 and 3.83 ppm due to six CH<sub>3</sub> protons of two *p*-CH<sub>3</sub>C<sub>6</sub>H<sub>4</sub>SO<sub>3</sub><sup>-</sup> anions and to eight OH protons of four H<sub>2</sub>O molecules, respectively. The <sup>1</sup>H NMR spectrum of complex **IIa** shows singlets at 2.57

Table 2  
Elemental analysis, selected IR,  $^1\text{H}$  and  $^{31}\text{P}$  NMR data

	Analysis	Elemental Analysis (%)			IR ( $\text{cm}^{-1}$ )	$^1\text{H}$ NMR $\delta$ (ppm)	$^{31}\text{P}$ NMR $\delta^*$ (ppm)
		C	H	S			
<b>Ia</b>	Found	57.33	4.85	6.11	3508, 3445 (OH, $\text{H}_2\text{O}$ )	2.30 s ( $\text{CH}_3$ , 6H, TsO)	34.43 s ( $\text{PPh}_3$ )
	Calculated	57.44	5.01	6.13	1227, 1033, 1008 ( $\text{SO}_3$ , $p\text{-CH}_3\text{C}_6\text{H}_4\text{SO}_3$ )	3.83 s (OH, 8H, $\text{H}_2\text{O}$ ) 6.97–7.73 m ( $\text{C}_6\text{H}_5$ , 38H, $\text{PPh}_3$ and TsO)	
<b>IIa</b>	Found	53.62	4.70	7.57	3534, 3489 (OH, $\text{H}_2\text{O}$ )	2.57 s ( $\text{CH}_3$ , 6H, $\text{CH}_3\text{SO}_3$ )	34.48 s ( $\text{PPh}_3$ )
	Calculated	53.25	4.70	7.48	1233, 1036, 1009 ( $\text{SO}_3$ , $\text{CH}_3\text{SO}_3$ )	4.79 s (OH, 4H, $\text{H}_2\text{O}$ ) 7.24–7.50 m ( $\text{C}_6\text{H}_5$ , 30H, $\text{PPh}_3$ )	
<b>Ib</b>	Found	59.71	4.73	6.61	1253, 1025, 1002	2.06 s ( $\text{CH}_3$ , 6H, TsO)	33.91 s ( $\text{PPh}_3$ )
	Calculated	61.60	4.55	6.58	( $\text{SO}_3$ , $p\text{-CH}_3\text{C}_6\text{H}_4\text{SO}_3$ )	6.77–8.03 m ( $\text{C}_6\text{H}_5$ , 38H, $\text{PPh}_3$ and TsO)	
<b>IIb</b>	Found	55.67	4.27	8.10	1265, 1026, 1001	2.46 s ( $\text{CH}_3$ , 6H, $\text{CH}_3\text{SO}_3$ )	33.70 s ( $\text{PPh}_3$ )
	Calculated	55.58	4.42	7.81	( $\text{SO}_3$ , $\text{CH}_3\text{SO}_3$ )	7.23–7.53 m ( $\text{C}_6\text{H}_5$ , 30H, $\text{PPh}_3$ )	

Abbreviations: s, singlet; m, multiplet; TsO,  $p\text{-CH}_3\text{C}_6\text{H}_4\text{SO}_3$ .  $^1\text{H}$  and  $^{31}\text{P}$  NMR spectra for **Ia** and **Ib** were taken in  $\text{CD}_3\text{COCD}_3$  and for **IIa** and **IIb** in  $\text{CDCl}_3$ . \* $\delta$  ( $^{31}\text{P}$ ) values in ppm from external 85%  $\text{H}_3\text{PO}_4$ , downfield shifts being taken as positive.

and 4.79 ppm assigned to six  $\text{CH}_3$  protons of two  $p\text{-CH}_3\text{SO}_3^-$  anions and to the four OH protons of two  $\text{H}_2\text{O}$  molecules, respectively.

Fig. 1 shows the thermogram of **Ia**: the first thermogravimetric step, accompanied by an endothermic DTA signal at 66.51  $^\circ\text{C}$ , is attributed to the loss of two molecules of water of crystallization, for which a theoretical mass loss of 3.44% is calculated, in agreement with the observed value of 3.30%. The endothermic DTA signals at 77.38 and 98.97  $^\circ\text{C}$  are attributed to the loss of two molecules of coordinated water, for which a theoretical mass loss of 1.72% is calculated, in agreement with the observed value of 1.40% and 1.70%, respectively. The thermogram confirms the presence of

two molecules of  $\text{H}_2\text{O}$  coordinated to the metal and of two molecules of  $\text{H}_2\text{O}$  of crystallization.

Fig. 2 shows the DTA analysis of complex **IIa**: only two endothermic signals are present at 66.51 and 75.11  $^\circ\text{C}$ , which correspond to the loss of two molecules of water with a mass loss of 2.10% and 2.00%, in agreement with the calculated theoretical value of 2.10%. Thus, the thermogram confirms the presence of two molecules of water. The comparison with the attribution just reported for **Ia** does not allow to establish unambiguously whether both molecules are coordinated, as in the case shown by the X-ray structure of **IIa**· $2\text{CH}_2\text{Cl}_2$ . The different TA behavior of the coordinated water molecules in the two complexes might be ascribed at least

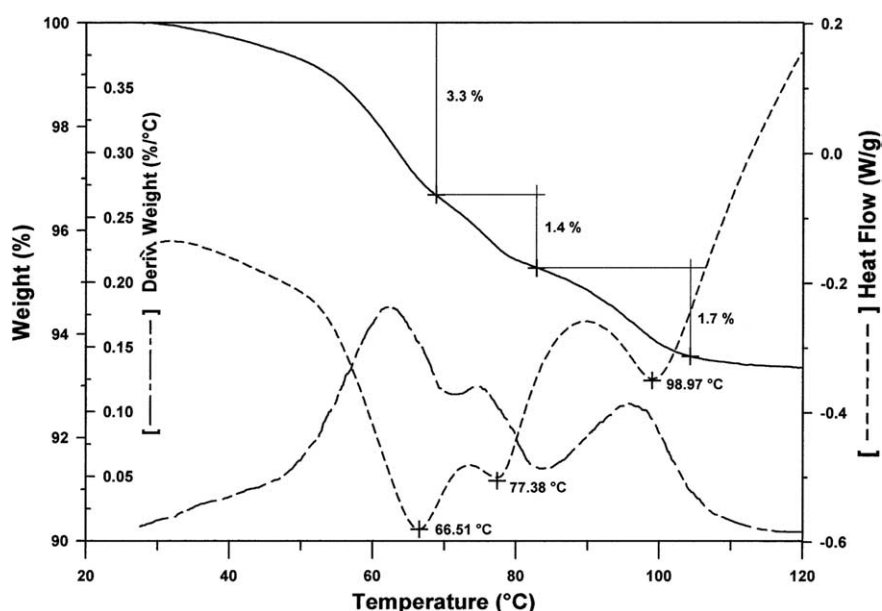


Fig. 1. Thermogravimetric analysis of complex **Ia**.

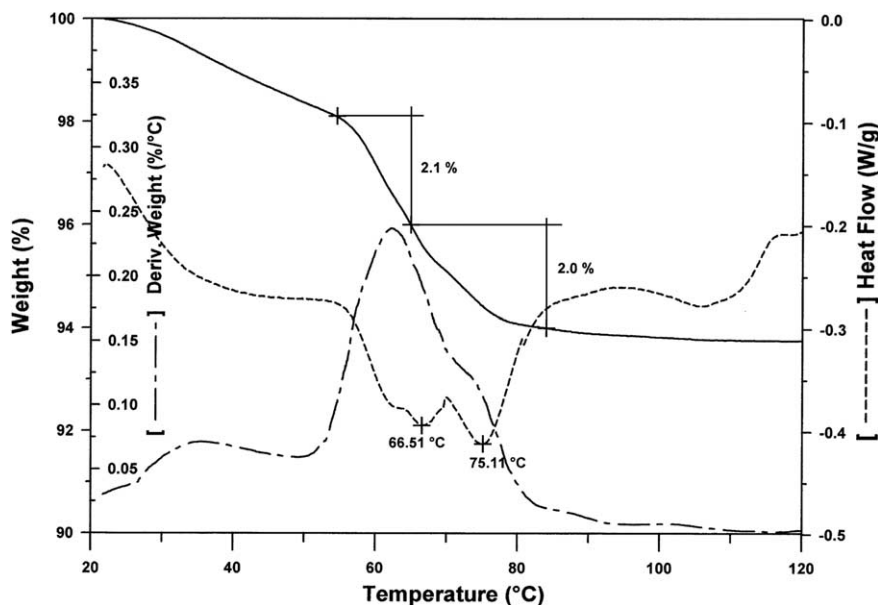


Fig. 2. Thermogravimetric analysis of complex **IIa**.

partially to the influence of intermolecular interactions. In fact, in **IIa** · 2CH<sub>2</sub>Cl<sub>2</sub> the coordinated water molecules are involved in a H-bond network; the latter is lacking in **Ia** (see Section 3.2).

### 3.2. X-ray structure analysis of the complexes **Ia** and **IIa** · 2CH<sub>2</sub>Cl<sub>2</sub>

The ORTEP [30] molecular structures of the two complexes, together with the numbering system employed, are depicted in Figs. 3 and 4; selected bond lengths and angles for both **Ia** and **IIa** · 2CH<sub>2</sub>Cl<sub>2</sub> are reported in Table 3.

The solid-state investigation of **Ia** revealed that the two *p*-toluenesulfonato units do not belong to the palladium coordination sphere, but they act as counter anions of the dicationic complex, in which the metal atom is surrounded in a square planar environment realized by two water molecules and two triphenylphosphine moieties that are *cis* to each other. The atoms in the basal plane P(1)–P(2)–O(1)–O(2) are roughly coplanar within 0.09 Å, with the Pd center deviating by 0.03 Å. The bond angles about Pd are around 90°; the largest deviations are shown by P(1)–Pd–P(2), 97.6(1)°, and O(1)–Pd–P(2), 84.1(1)°. The O(1)–Pd–P(1) angle measures 176.9(1)°, whereas O(2)–Pd–P(2) is 169.4(1)°.

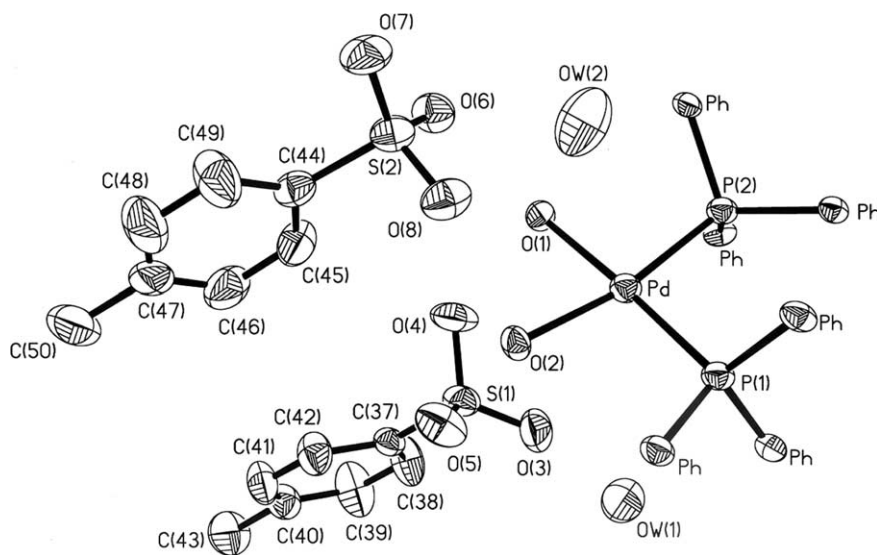


Fig. 3. A drawing of the complex **Ia** with the adopted numbering scheme. Ellipsoids have been drawn at the 40% probability level; the hydrogen atoms and the phenyl rings of the PPh<sub>3</sub> units have been omitted for clarity.

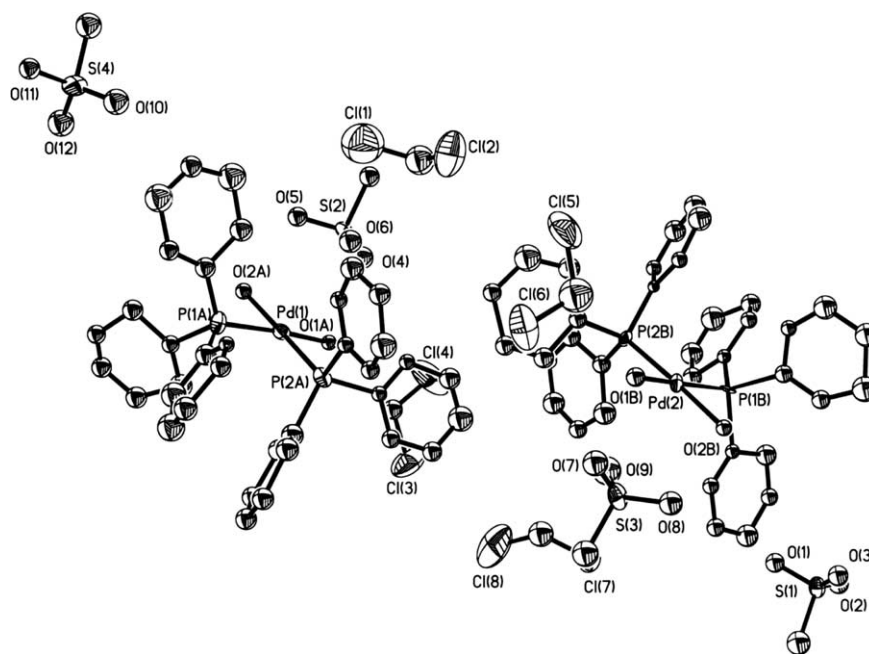


Fig. 4. The content of the unit cell of complex **IIa** · 2CH<sub>2</sub>Cl<sub>2</sub>. Ellipsoids have been drawn at the 40% probability level.

Table 3  
Selected bond distances (Å) and bond angles (°) for **Ia** and **IIa** · 2CH<sub>2</sub>Cl<sub>2</sub>

<b>I</b>			
Pd–P(1)	2.258(1)	Pd–P(2)	2.263(1)
Pd–O(1)	2.146(3)	Pd–O(2)	2.129(3)
P(1)–C(1)	1.812(4)	P(1)–C(7)	1.803(5)
P(1)–C(13)	1.797(5)	P(2)–C(19)	1.805(4)
P(2)–C(25)	1.817(5)	P(2)–C(31)	1.816(4)
S(1)–O(3)	1.432(4)	S(1)–O(4)	1.452(3)
S(1)–O(5)	1.467(4)	S(1)–C(37)	1.774(5)
S(2)–O(6)	1.476(3)	S(2)–O(7)	1.452(3)
S(2)–O(8)	1.483(3)	S(2)–C(44)	1.778(6)
O(1)–Pd–O(2)	87.4(1)	P(2)–Pd–O(2)	169.4(1)
P(2)–Pd–O(1)	84.1(1)	P(1)–Pd–O(2)	91.2(1)
P(1)–Pd–O(1)	176.9(1)	P(1)–Pd–P(2)	97.6(1)
O(5)–S(1)–C(37)	105.7(2)	O(4)–S(1)–C(37)	105.2(2)
O(4)–S(1)–O(5)	111.8(2)	O(3)–S(1)–C(37)	108.5(2)
O(3)–S(1)–O(5)	112.1(3)	O(3)–S(1)–O(4)	112.9(2)
O(8)–S(2)–C(44)	104.8(2)	O(7)–S(2)–C(44)	106.1(3)
O(7)–S(2)–O(8)	113.5(2)	O(6)–S(2)–C(44)	106.4(2)
O(6)–S(2)–O(8)	111.4(2)	O(6)–S(2)–O(7)	113.9(2)
<b>IIa</b> · 2CH <sub>2</sub> Cl <sub>2</sub>			
<b>(A)</b>		<b>(B)</b>	
Pd(1)–P(1A)	2.25(1)	Pd(2)–P(1B)	2.28(1)
Pd(1)–P(2A)	2.25(1)	Pd(2)–P(2B)	2.25(1)
Pd(1)–O(1A)	2.11(2)	Pd(2)–O(1B)	2.12(2)
Pd(1)–O(2A)	2.15(2)	Pd(2)–O(2B)	2.09(2)
P(1A)–Pd(1)–P(2A)	96.1(3)	P(1B)–Pd(2)–P(2B)	96.7(3)
P(1A)–Pd(1)–O(1A)	169.4(6)	P(1B)–Pd(2)–O(1B)	170.1(7)
P(1A)–Pd(1)–O(2A)	83.8(6)	P(1B)–Pd(2)–O(2B)	83.4(6)
P(2A)–Pd(1)–O(1A)	91.0(6)	P(2B)–Pd(2)–O(1B)	91.5(7)
P(2A)–Pd(1)–O(2A)	179.1(7)	P(2B)–Pd(2)–O(2B)	178.1(7)
O(1A)–Pd(1)–O(2A)	89.0(8)	O(1B)–Pd(2)–O(2B)	88.6(8)

thus deviating appreciably from linearity. Despite these deviations, the distortion of the square-planar arrangement is little overall. In fact, the sum of the bond angles about Pd is 360.3(1)°, while the tetrahedral distortion, measured by the dihedral angle between the P(1)–Pd–P(2) and the O(1)–Pd–O(2) planes, is limited to 6.5°.

A search for Pd(II) complexes of general formula L<sub>2</sub>PdP<sub>2</sub> (P = monodentate neutral phosphorous ligand, L = monodentate ligand) in the Cambridge Structural Database [31] revealed 22 structures where the two phosphorous ligands adopt the *cis* arrangement. The latter does not appear hence particularly unusual; actually, the studies of Nelson and co-workers [32–34] indicate that if the steric effects of the phosphorous ligands are not too large, the *cis* isomer is thermodynamically more stable than the *trans* one, especially in the presence of favorable solute–solvent interactions. In these cases, there is some degree of distortion of the square planar environment towards the tetrahedral one, defined as pseudotetrahedrality [32].

In the present study, the tetrahedral distortion is limited to 6.5°, a value similar to that of 6.1° found by Mak and co-workers [35] in *cis*-[(Ph<sub>2</sub>Ppym)<sub>2</sub>PdCl<sub>2</sub>] · 1/2CH<sub>2</sub>Cl<sub>2</sub> and smaller than those found either by Jensen and co-workers [36] in *cis*-PdCl<sub>2</sub>[P(CH<sub>3</sub>)<sub>3</sub>]<sub>2</sub> and Romero et al. [37] in [*cis*-Pd(8-BzTT)<sub>2</sub>(PPh<sub>3</sub>)<sub>2</sub>] (8.9° and 13.2°, respectively). The little steric demand of the two coordinated water molecules in the present complex, if compared to the bulk of other ligands [35–37], also contributes to keep the tetrahedral distortion to a minimum and help in stabilizing the *cis* geometry.

It is also interesting to note that, despite the rather large number of reports about Pd(II)–aqua complexes in

the Cambridge Structural Database, we could find only six mono-aqua and five diaqua-*cis*-diphosphine palladium(II) derivatives [24,29,38–42]. In all these structures but one [29] the phosphorous atom belongs to a chelate diphosphine ligand. Furthermore, one of such structures appears to be suffering from some disorder [38], whereas compound [29] turned out to have the Pd center surrounded by the same coordination environment as in both **Ia** and **IIa** · 2CH<sub>2</sub>Cl<sub>2</sub>. Table 4 reports a detailed comparison of the main geometric features of these complexes.

The Pd–P distances in the reported complexes range between 2.206(1) Å in [Pd(H<sub>2</sub>O){1,3-bis-DTBOEPP}](BF<sub>4</sub>)<sub>2</sub> (DTBOEPP = di(2-*t*-butoxyethyl)phosphino-propane) [41] and 2.279(2) Å in [Pd(H<sub>2</sub>O)<sub>2</sub>(dppomf)<sub>2</sub>](OTf)<sub>2</sub> [40] (mean value = 2.25 Å). In **Ia**, the Pd–P distances are 2.258(1) and 2.263(1) Å, slightly above the average and similar to those found in the nearly identical complex [Pd(H<sub>2</sub>O)<sub>2</sub>(PPh<sub>3</sub>)<sub>2</sub>](OTf)<sub>2</sub> [29] (2.250(1)

and 2.277(1) Å) and in [Pd(H<sub>2</sub>O)<sub>2</sub>(dppf)](OTf)<sub>2</sub> [41] (2.263(1) and 2.267(1) Å), where the ligand is 1,1'-bis(diphenylphosphino)ferrocene. In any case, these values fit nicely in the range reported for 102 square planar Pd(II) complexes deposited within the Cambridge Structural Database. The Pd–O distances in Table 4 range between 2.106(4) Å in [Pd(OTf)(H<sub>2</sub>O)(dppp)](OTf) [25] and 2.254(3) Å in [Pd(H<sub>2</sub>O){1,3-bis-DTBOEPP}](BF<sub>4</sub>)<sub>2</sub> [40] (mean value = 2.14 Å). In **Ia**, Pd–O distances are 2.146(3) and 2.129(3) Å, just about the reported average and in good agreement with the values reported for [Pd(H<sub>2</sub>O)<sub>2</sub>(PPh<sub>3</sub>)<sub>2</sub>](OTf)<sub>2</sub> [29]. P–C<sub>ph</sub> distances, with an average value of 1.808 Å, do not show instead any special feature and remain within the range of reported data.

With respect to the bond angles listed in Table 4, the P(1)–Pd–P(2) angle ranges between 88.61(4)° in [Pd(*p*-CH<sub>3</sub>C<sub>6</sub>H<sub>4</sub>SO<sub>3</sub>)(H<sub>2</sub>O)(dppp)](*p*-CH<sub>3</sub>C<sub>6</sub>H<sub>4</sub>SO<sub>3</sub>) [24] and 101.32(5)° in [Pd(H<sub>2</sub>O)<sub>2</sub>(dppomf)<sub>2</sub>](OTf)<sub>2</sub> [41] (mean

Table 4  
Geometrical parameters of reported mono-aqua- and diaqua-*cis*-diphosphine Pd(II) derivatives

	Pd–P	Pd–O	P(1)–Pd–P(2)	O(1)–Pd–O(2)
<i>Monoaqua complexes</i>				
[Pd(H <sub>2</sub> O)(dppp)(OTs)](OTs) [24]	2.236(1)	2.138(4)	88.61(4)	85.9(1)
	2.236(1)	2.152(3) <sup>a</sup>		
[Pd(H <sub>2</sub> O)(dppp)(OTf)](OTf) [25]	2.237(1)	2.106(4)	90.98(4)	86.1(2)
	2.228(1)	2.159(3) <sup>b</sup>		
[Pd(H <sub>2</sub> O){( <i>S</i> )-MeO-BIPHEP}(THF)](OTf) <sub>2</sub> [39]	2.248(4)	2.147(9)	90.7(2)	87.1(4)
	2.256(4)	2.13(1) <sup>c</sup>		
[Pd(H <sub>2</sub> O){1,3-bis-DTBOEPP}](BF <sub>4</sub> ) <sub>2</sub> [40]	2.206(1)	2.154(3)	89.71(5)	96.4(1)
	2.233(1)	2.254(3) <sup>d</sup>		
[Pd(H <sub>2</sub> O)(dippf)(NCMe)](OTf) <sub>2</sub> · 2H <sub>2</sub> O [42] <sup>e</sup>	2.267	2.156	101.26	
	2.270			
[Pd(H <sub>2</sub> O)(( <i>R</i> )-BINAP)(NCMe)](OTf) <sub>2</sub> · 1/2H <sub>2</sub> O [42] <sup>e</sup>	2.255	2.136	91.15	
	2.245			
<i>Diaqua complexed</i>				
[Pd(H <sub>2</sub> O) <sub>2</sub> (( <i>R</i> )-Tol-BINAP)](BF <sub>4</sub> ) <sub>2</sub> · 2H <sub>2</sub> O [38]	2.257(3)	2.159(9)	91.4(1)	87.0(4)
	2.235(3)	2.160(9)		
[Pd(H <sub>2</sub> O) <sub>2</sub> (dppp)](OTf) <sub>2</sub> [25]	2.226(1)	2.127(2)	90.33(2)	87.66(8)
	2.231(1)	2.135(2)		
[Pd(H <sub>2</sub> O) <sub>2</sub> (PPh <sub>3</sub> ) <sub>2</sub> ](OTf) <sub>2</sub> [29]	2.250(1)	2.130(2)	94.94(2)	87.06(7)
	2.277(1)	2.119(2)		
[Pd(H <sub>2</sub> O) <sub>2</sub> (PPh <sub>3</sub> ) <sub>2</sub> ](OTs) <sub>2</sub> · 2H <sub>2</sub> O [this work]	2.258(1)	2.146(3)	97.6(1)	87.4(1)
	2.263(1)	2.129(3)		
[Pd(H <sub>2</sub> O) <sub>2</sub> (PPh <sub>3</sub> ) <sub>2</sub> ](OSO <sub>2</sub> Me) <sub>2</sub> · 2 CH <sub>2</sub> Cl <sub>2</sub> [this work] <sup>f</sup>	2.25(1)	2.11(1)	96.1(3)	89.0(8)
	2.25(1)	2.15(1)		
	2.25(2)	2.12(2)	96.7(3)	88.6(8)
	2.28(2)	2.09(2)		
[Pd(H <sub>2</sub> O) <sub>2</sub> (dppf)](OTf) <sub>2</sub> [41]	2.263(1)	2.117(3)	96.38(4)	87.6(1)
	2.267(1)	2.132(3)		
[Pd(H <sub>2</sub> O) <sub>2</sub> (dppomf) <sub>2</sub> ](OTf) <sub>2</sub> [41]	2.279(2)	2.117(4)	101.32(5)	87.0(2)
	2.271(2)	2.169(4)		
Mean	2.25	2.14	94.1	88.1

<sup>a</sup> Refers to the *p*-toluenesulfonate oxygen.

<sup>b</sup> Refers to the trifluoromethanesulfonate oxygen.

<sup>c</sup> Refers to the tetrahydrofuran oxygen.

<sup>d</sup> Refers to the butoxyethyl oxygen.

<sup>e</sup> Bond distances and angles extracted from the Cambridge Structural Database; standard deviations unavailable.

<sup>f</sup> Low quality of diffraction data.

value = 94.1°). In the complex described in this work, the P(1)–Pd–P(2) angle measures 97.6(1)°. This is the third largest value recorded so far for aqua *cis*-diphosphine palladium(II) derivatives and is also slightly larger than that found in the almost equal [Pd(H<sub>2</sub>O)<sub>2</sub>(PPh<sub>3</sub>)<sub>2</sub>](OTf)<sub>2</sub> [29] (94.94(2)°). On the other side, the O(1)–Pd–O(2) angle does not change very much (mean value = 88.1°), but for complex [Pd(H<sub>2</sub>O){1,3-bis-DTBOEPP}](BF<sub>4</sub>)<sub>2</sub> [41] (96.4(1)°). In **Ia**, it measures 87.4(1)° and agrees well with the values reported for the other diaqua complexes.

Interestingly, despite the presence of two hydration water molecules and of two *p*-toluenesulfonato anions, a situation similar to that reported by Stang et al. [25], no efficient intermolecular interactions are present in the complex. In fact, the closest intermolecular contacts between the complexed water molecules and the oxygen atoms of the sulfonato groups are greater than 2.6 Å; the distances between the OW1 and OW2 atoms of the hydration water molecules and the oxygen atoms of the sulfonato groups are even larger.

The X-ray investigation of **IIa** · 2CH<sub>2</sub>Cl<sub>2</sub> showed that in the acentric triclinic cell there are two independent (**A** and **B**) [Pd(H<sub>2</sub>O)<sub>2</sub>(PPh<sub>3</sub>)<sub>2</sub>]<sup>2+</sup> units, together with two methanesulfonato counter anions and two crystallization CH<sub>2</sub>Cl<sub>2</sub> molecules. All the molecules suffer from high thermal motions and this is especially true for the atoms belonging to the dichloromethane molecules. Actually, the solvent molecules are the main responsible for the poor stability of the crystal and their presence

leads to the irremediable disruption of the crystal structure. In just few hours, an amorphous dark residue replaces the starting needle-shaped yellow crystals and the process obviously spoils the X-ray data collection.

The bad quality of the diffraction data reduced the information obtained from the diffraction experiment and in effect the most valuable result of the crystallographic determination is the stereochemistry of the complex. The palladium coordination sphere of both [Pd(H<sub>2</sub>O)<sub>2</sub>(PPh<sub>3</sub>)<sub>2</sub>]<sup>2+</sup> units shows the same environment found either in complex **Ia** or [Pd(H<sub>2</sub>O)<sub>2</sub>(PPh<sub>3</sub>)<sub>2</sub>](OTf)<sub>2</sub> [29]; some caution is instead necessary when discussing bond lengths and angles (Table 4). Bond angles around the metal centers appear close to 90°; hence, also in **IIa** · 2CH<sub>2</sub>Cl<sub>2</sub> the overall distortion of the square-planar arrangement appears to be little, with the sum of the bond angles about the two palladium atoms being just about 360°.

Opposite to what has been found for complex **Ia**, the coordination water molecules of the two independent [Pd(H<sub>2</sub>O)<sub>2</sub>(PPh<sub>3</sub>)<sub>2</sub>]<sup>2+</sup> units are engaged in some rather loose hydrogen bonds (Fig. 5). In particular, the O(1A) and O(2A) oxygens are bonded, respectively, to the O(10) and O(11) atoms of a methanesulfonato group belonging to a different unit placed at *x*, 1 + *y*, *z*, with O···O contact distances of 2.56 and 2.60 Å, respectively. In the same way, the O(1B) and O(2B) atoms are linked to the O(1) and O(2) oxygens of a second methanesulfonato moiety, again placed at *x*, 1 + *y*, *z*, with O···O contact distances of 2.68 and 2.59 Å, respectively.

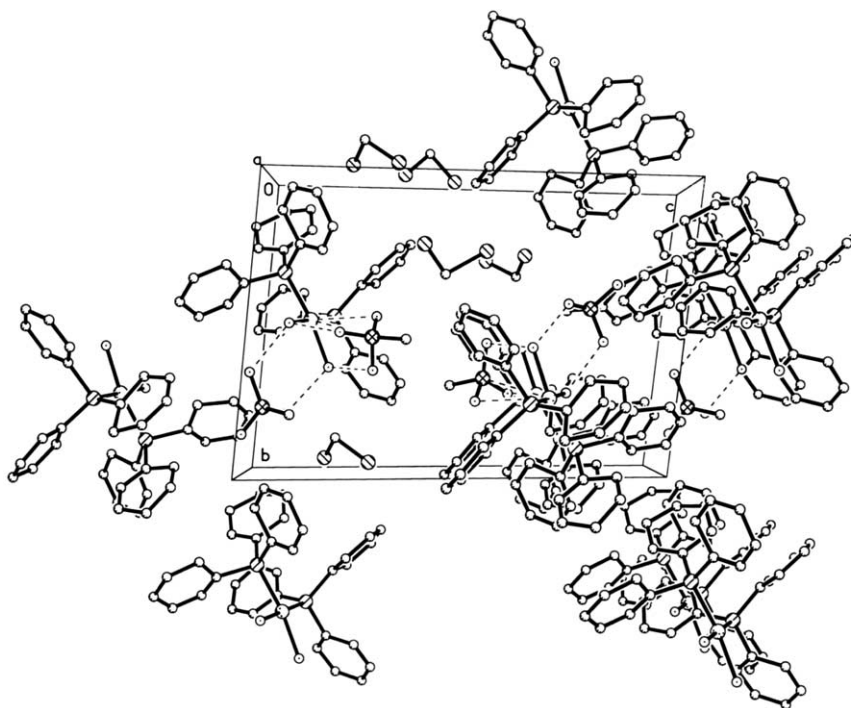


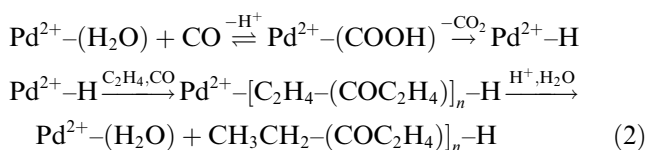
Fig. 5. A cell packing diagram illustrating the hydrogen bond network in complex **IIa** · 2CH<sub>2</sub>Cl<sub>2</sub>.

The hydrogen bond network is completed by some interactions taking place within the same crystallographic unit and linking in turn O(1A) and O(4), O(2A) and O(5), O(1B) and O(7), O(2B) and O(8). The O...O contact distances are of 2.88, 2.75, 2.67 and 2.65 Å, respectively, just a little longer than those mentioned above.

The hydrogen bond network of **IIa**·2CH<sub>2</sub>Cl<sub>2</sub> looks similar to those described in [Pd(OTf)(H<sub>2</sub>O)(dppp)]-(OTf) [25] and in the nearly identical complex [Pd(H<sub>2</sub>O)<sub>2</sub>(PPh<sub>3</sub>)<sub>2</sub>](OTf)<sub>2</sub> [29]. In particular, both coordinate water molecules are doubly hydrogen-bonded to the two methanesulfonato anions, and the two water molecules are each hydrogen-bonded to different anions rather than to the same one. This hydrogen bond pattern is likely to afford some stability to the crystal structure of **IIa**·2CH<sub>2</sub>Cl<sub>2</sub>.

### 3.3. Catalytic activity of **Ia** in the carbonylation of ethene

The catalytic activity of complex **Ia** has been tested at r.t., in chloroform as solvent and in the presence of four equivalents of CH<sub>3</sub>CN, in order to get close to the conditions reported by Sen and Lai [6,7], which used as precursor the system [Pd(CH<sub>3</sub>CN)<sub>4</sub>](BF<sub>4</sub>)<sub>2</sub> in combination with two equivalents of PPh<sub>3</sub>. After ca. 20 h, there was production of 25 g of polymer/g of Pd. <sup>13</sup>C NMR analysis shows average *n* = 27 and that only keto end-groups CH<sub>3</sub>CH<sub>2</sub>CO– are present. Moreover, catalysis occurs with formation of CO<sub>2</sub>. Thus, the polymerization can be schematized as follows: (i) the Pd(II)–hydride that starts the catalysis forms upon interaction of H<sub>2</sub>O with CO on the metal center and decarboxylation of the resulting Pd(II)–carboxy species; (ii) multiple sequential insertion of C<sub>2</sub>H<sub>4</sub> and CO; and (iii) protonolysis of a Pd(II)–C bond of the growing chain giving the polyketone and Pd(II) species back to the catalytic cycle. It is interesting to underline that with the precursor used by Lai and Sen [7], water is not introduced by the complex and that the molecular weight of the polyketone is so high not to allow the identification of the end groups.



The capability of complex **Ia** to catalyze the copolymerization may be related to its *cis* geometry [1]. However, we have found that also the acyl complex *trans*-[Pd(COEt)(*p*-CH<sub>3</sub>C<sub>6</sub>H<sub>4</sub>SO<sub>3</sub>)(PPh<sub>3</sub>)<sub>2</sub>], a possible intermediate in the polymerization process that may form after the insertion of just one molecule of ethene and of CO into the Pd(II)–H species, in the presence of four equivalents of CH<sub>3</sub>CN catalyzes the formation of

the polyketone (ca. 2 g of polymer/g of Pd). It is likely that *cis*–*trans* isomerization occurs even at r.t. and that catalysis is promoted by the *cis* isomer.

The catalytic activity of **Ia** to methyl propanoate has been also tested in the presence of H<sub>2</sub>O and of *p*-CH<sub>3</sub>C<sub>6</sub>H<sub>4</sub>SO<sub>3</sub>H, which have been proven to promote the catalysis, and in the presence also of PPh<sub>3</sub> to stabilize the catalytic system [11]. In MeOH at 80 °C and 4.5 MPa (CO/ethene = 1/1), **Ia** or **IIa** affords methyl propanoate with a TOF of ca. 420 h<sup>-1</sup> in the presence of 800 ppm of H<sub>2</sub>O and with a Pd/PPh<sub>3</sub>/*p*-CH<sub>3</sub>C<sub>6</sub>H<sub>4</sub>SO<sub>3</sub>H ratio of 1/8/8, as found when [Pd(*p*-CH<sub>3</sub>C<sub>6</sub>H<sub>4</sub>SO<sub>3</sub>)<sub>2</sub>(PPh<sub>3</sub>)<sub>2</sub>] or *trans*-[Pd(COEt)(*p*-CH<sub>3</sub>C<sub>6</sub>H<sub>4</sub>SO<sub>3</sub>)(PPh<sub>3</sub>)<sub>2</sub>] are used as precursors [11,14]. The formation of CO<sub>2</sub> during the catalysis suggests that it starts via a Pd(II)–H species. In this case, after the insertion of just one molecule of C<sub>2</sub>H<sub>4</sub> and of CO with formation of Pd(II)–acyl intermediate, methanolysis to methyl propanoate interrupts the chain growing.

### References

- [1] E. Drent, P.H.M. Budzelaar, Chem. Rev. 96 (1996) 663.
- [2] G. Kiss, Chem. Rev. 101 (2001) 3435.
- [3] R.A.M. Robertson, D.J. Cole-Hamilton, Coord. Chem. Rev. 225 (2002) 67.
- [4] E. Drent (Shell), EP 121 965, 1984.
- [5] E. Drent, J.A.M. Van Broekhoven, M.J. Doyle, J. Organomet. Chem. 417 (1991) 235.
- [6] A. Sen, T.-W.T. Lai, J. Am. Chem. Soc. 104 (1982) 3520.
- [7] T.-W. Lai, A. Sen, Organometallics 3 (1984) 866.
- [8] A. Sen, Acc. Chem. Res. 26 (1993) 303.
- [9] A. Seayad, A.A. Kelkar, L. Toniolo, R.V. Chaudhari, J. Mol. Catal. 151 (2000) 47.
- [10] A. Seayad, S. Jayasree, K. Damodaran, L. Toniolo, R.V. Chaudhari, J. Organomet. Chem. 601 (2000) 100.
- [11] A. Vavasori, G. Cavinato, L. Toniolo, J. Mol. Catal. 176 (2001) 11.
- [12] A. Vavasori, G. Cavinato, L. Toniolo, J. Mol. Catal. 191 (2003) 9.
- [13] G. Cavinato, A. Vavasori, L. Toniolo, F. Benetollo, Inorg. Chim. Acta 343 (2003) 183.
- [14] G. Cavinato, L. Toniolo, A. Vavasori, J. Mol. Catal., in press.
- [15] J. Knifton, J. Org. Chem. 41 (1976) 2885.
- [16] G. Cavinato, L. Toniolo, J. Organomet. Chem. 198 (1990) 187.
- [17] S. Otsuka, A. Nakamura, T. Yoshida, M. Naruto, K. Ataka, J. Am. Chem. Soc. 95 (1973) 3180.
- [18] D.M. Fenton, J. Org. Chem. 38 (1973) 3192.
- [19] D. Milstein, Acc. Chem. Res. 21 (1988) 428.
- [20] G.M. Sheldrick, SHELXTL/PC: Version 5.03, Siemens Analytical X-ray Instruments Inc., Madison, WI, 1994.
- [21] G.M. Sheldrick, SHELXL-93: Program for the Refinement of Crystal Structures, University of Göttingen, Germany, 1993.
- [22] B. Chiswell, L.M. Venanzi, J. Chem. Soc. A (1966) 1246.
- [23] P. Leoni, M. Sommovigo, M. Pasquali, S. Midollini, D. Braga, P. Sabatino, Organometallics 11 (1991) 1038.
- [24] F. Benetollo, R. Bertani, G. Bombieri, L. Toniolo, Inorg. Chim. Acta 233 (1995) 5.
- [25] P.J. Stang, D.H. Cao, G.T. Poulter, A.M. Arif, Organometallics 14 (1995) 1110.
- [26] U. Bohner, G. Zundel, J. Phys. Chem. 89 (1985) 1408.
- [27] G.J. Kubas, C.J. Burns, G.R.K. Khalsa, L.S. Van Der Sluys, G. Kiss, C.D. Hoff, Organometallics 11 (1992) 3390.

- [28] R.K. Merwin, D.M. Roddick, *J. Organomet. Chem.* 487 (1995) 69.
- [29] Z. Qin, M.C. Jennings, R.J. Puddephatt, *Inorg. Chim. Acta* 40 (2001) 6220.
- [30] C.K. Johnson, ORTEP, Report ORNL-5138, Oak Ridge National Laboratory, Oak Ridge, TN, 1976.
- [31] F.H. Allen, *Acta Crystallogr., Sect. B* 58 (2002) 380, Cambridge Crystallographic Database (Version 5.25 of November 2003).
- [32] J.J. MacDougall, J.H. Nelson, F. Mathey, J.J. Mayerle, *Inorg. Chem.* 19 (1980) 709.
- [33] J.J. MacDougall, E.M. Holt, P. de Meester, N.W. Alcock, F. Mathey, J.H. Nelson, *Inorg. Chem.* 19 (1980) 1439.
- [34] K.D. Redwine, W.L. Wilson, D.G. Moses, V.J. Catalano, J.H. Nelson, *Inorg. Chem.* 39 (2000) 3392.
- [35] S.-L. Li, Z.-Z. Zhang, B.-M. Wu, T.C.W. Mak, *Inorg. Chim. Acta* 255 (1997) 239.
- [36] G. Schultz, N.Yu. Subbotina, C.M. Jensen, J.A. Golen, I. Hargittai, *Inorg. Chim. Acta* 191 (1992) 85.
- [37] A. Romerosa, C. Lopez-Magana, M. Saoud, S. Manas, E. Colacio, J. Suarez-Varela, *Inorg. Chim. Acta* 307 (2000) 125.
- [38] M. Sodeoka, R. Tokunoh, F. Miyazaki, E. Hagiwara, M. Shibasaki, *Synlett* 463 (1997).
- [39] M. Sperrle, V. Gramlich, G. Consiglio, *Organometallics* 15 (1996) 5196.
- [40] E. Lindner, M. Schmid, P. Wegner, C. Nachtigal, M. Steimann, R. Fawzi, *Inorg. Chim. Acta* 296 (1999) 103.
- [41] O.V. Gusev, A.M. Kalsin, M.G. Peterleitner, P.P. Petrovskii, K.A. Lissenko, *Organometallics* 21 (2002) 3637.
- [42] K. Li, P.N. Norton, M.B. Hursthouse, K.K. Hii, *J. Organomet. Chem.* 665 (2003) 250.